Quantum Yields for NO_3 Photolysis between 570 and 635 nm

John J. Orlando,* Geoffrey S. Tyndall, Geert K. Moortgat,† and Jack G. Calvert

Atmospheric Chemistry Division, National Center for Atmospheric Research, Boulder, Colorado 80307

Received: April 27, 1993; In Final Form: August 12, 1993

Quantum yields for the production of $O(^3P)$ from the photolysis of NO_3 have been measured over the wavelength range 570–635 nm, using a pulsed laser photolysis–resonance fluorescence technique. Absolute $O(^3P)$ quantum yields were determined at selected wavelengths using O_3 photolysis to normalize for laser energy and detection sensitivity; the measured quantum yields were 1.06 ± 0.26 at 582 nm, 0.72 ± 0.18 at 590 nm, and 0.52 ± 0.13 at 603 nm. Combining these absolute yields with a series of relative measurements made as a function of wavelength, the $O(^3P)$ yield was found to be unity between 570 and 585 nm and to decrease in essentially linear fashion from 585 nm to near zero at 640 nm. Anomalously low $O(^3P)$ yields were noted in the strong absorption bands near 623 nm. In addition, NO has been detected as a minor product of NO_3 photolysis (quantum yield about 20%) near 590 nm. The data have been used to calculate atmospheric photolysis rates for (1) $NO_3 + h\nu \rightarrow NO_2 + O(^3P)$, $j_1 = 0.19\ s^{-1}$ and (2) $NO_3 + h\nu \rightarrow NO + O_2$, $j_2 = 0.016\ s^{-1}$. From the wavelength threshold for process 1, the $\Delta H_{f,298}$ for NO_3 was estimated to be 18 ± 1 kcal/mol.

Introduction

The role of the NO_3 radical as an oxidant in the earth's atmosphere has stimulated intense investigation into its thermodynamics, spectroscopy, kinetics, and photochemistry.[1] Because of its strong absorption throughout the visible region of the spectrum, photolysis of NO_3 is a major loss process in the daytime atmosphere. At present, a qualitative picture of the photochemistry and photophysics of NO_3 has been obtained. The visible absorption feature consists of a series of diffuse absorption bands extending throughout the visible region of the spectrum (400–680 nm). Absorption cross sections in this region have been measured by numerous investigators,[2–11] with a currently recommended[1] 298 K value of $(2.1 \pm 0.2) \times 10^{-17}$ cm^2 molecule^{-1} for the strong 0–0 band near 662 nm. The recommended room temperature cross sections over the entire visible absorption system[1] are based on the data of Sander,[8] normalized to the value of 2.1×10^{-17} cm^2 molecule^{-1} at 662 nm.

A number of photodissociation channels are energetically allowed in the wavelength range of interest:

$$NO_3 + h\nu \rightarrow NO_2(X^2A_1) + O(^3P), \quad \lambda < 580\ \text{nm} \qquad (1)$$

$$\rightarrow NO(X^2\Pi) + O_2(X^3\Sigma_g^-), \quad \lambda < 8000\ \text{nm} \qquad (2a)$$

$$\rightarrow NO(X^2\Pi) + O_2(a^1\Delta_g), \quad \lambda < 1100\ \text{nm} \qquad (2b)$$

$$\rightarrow NO(X^2\Pi) + O_2(b^1\Sigma_g^+), \quad \lambda < 700\ \text{nm} \qquad (2c)$$

Quantum yields for NO_3 have been reported by Graham and Johnston[2] and Magnotta and Johnston.[12] Both dissociation channels 1 and 2 appear to occur, leading to the production of NO_2 and NO. The electronic state(s) of the O_2 photoproduct obtained from reaction 2 is (are) not known. While Graham and Johnston[2] inferred average quantum yields from broad-band photolysis, Magnotta and Johnston[12] made quantitative measurements of both the O and NO photoproducts using laser photolysis. The quantum yield for (1), ϕ_1, appears to be fairly constant from about 470 to 585 nm and then decreases to zero near 640 nm, while the quantum yield for (2), ϕ_2, rises from zero near 585 nm, peaks near 592 nm, and also falls to zero near 640 nm. However, systematic errors seem to exist in this data set since the sum of the reported quantum yields exceeds unity below 595 nm when the currently recommended NO_3 cross sections are employed. Although not measured on an absolute scale, fluoresence data[13–15] are qualitatively consistent with the photochemical measurements. Fluorescence yields appear to be large and approximately constant between 662 and 625 nm and decrease to near zero near 600 nm. No fluorescence is observed for wavelengths below 595 nm.

In this paper, a quantitative determination of the quantum yields of NO_3 as a function of wavelength is reported. Relative $O(^3P)$ yields are measured between 570 and 635 nm and are placed on an absolute scale using O_3 photolysis to calibrate for laser energy and $O(^3P)$ detection sensitivity. Approximate quantum yields for NO production from NO_3 photolysis are also reported at selected wavelengths. The results are compared to previously published quantum yields and are discussed in terms of the rate and products of NO_3 photolysis in the atmosphere. The heat of formation of NO_3 is also estimated from the wavelength threshold for $O(^3P)$ production, and comparisons are made to previous values.

Experimental Section

A schematic of the experimental apparatus is shown in Figure 1. The system consists of a microwave discharge/flow tube for NO_3 generation, an O_3 flow/monitoring system, an excimer-pumped pulsed dye laser for NO_3 and O_3 photolysis, resonance lamps ($O(^3P)$ or NO) to excite photoproduct fluorescence, and a photomultiplier tube (PMT) system for collection of the time-resolved fluorescence signal following the laser pulse.

The discharge-flow tube system for NO_3 generation has been described previously.[16,17] Briefly, NO_3 was produced from the reaction of F atoms with excess HNO_3:

$$F + HNO_3 \rightarrow NO_3 + HF \qquad (3)$$

with $k_3 = 2.3 \times 10^{-11}$ cm^3 s^{-1}.[18] The main carrier gas in the flow tube (i.d. 20.2 mm) was He (flow rate between 200 and 500 sccm), and the flow tube pressure was maintained between 2 and 5 Torr for most experiments, giving linear flow velocities between 500 and 750 cm s^{-1}. The HNO_3 was added to the flow tube by bubbling He (50 sccm) through a 1:2 mixture of 65% HNO_3 in

† Permanent address: Atmospheric Chemistry Division, Max-Planck-Institut für Chemie, Postfach 3060, D-55020 Mainz, Germany.

• Abstract published in *Advance ACS Abstracts*, October 1, 1993.

0022-3654/93/2097-10996$04.00/0

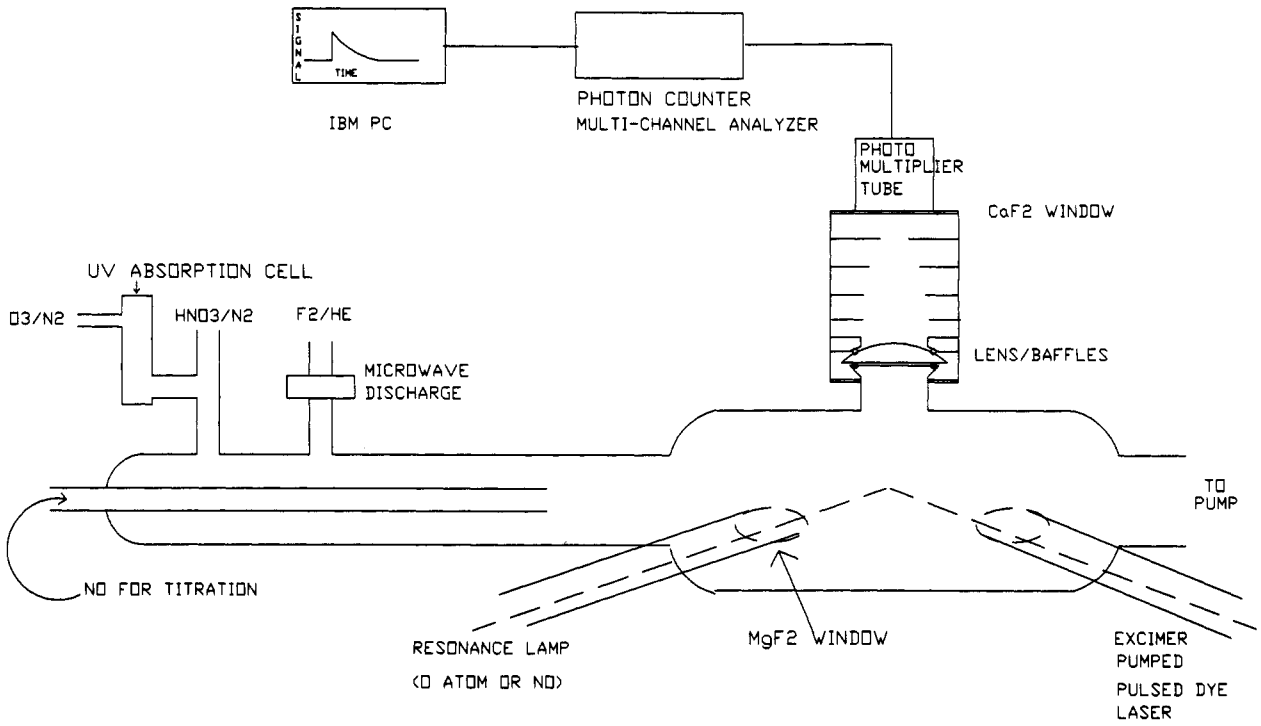

Figure 1. Schematic of experimental apparatus.

concentrated H_2SO_4. Infrared analysis has shown the levels of H_2O in the flow to be less than 1% of the HNO_3.[16] F atoms were generated in a side arm located 50 cm downstream of the HNO_3 addition port. They were produced in a microwave discharge in F_2/He (1–3 sccm of a 1:20 mixture), to which an additional He flow (35–75 sccm) was added. Typically, initial flow tube concentrations were (2–5) $\times 10^{15}$ cm^{-3} for HNO_3 and (1–5) $\times 10^{13}$ cm^{-3} for F_2, which resulted in NO_3 concentrations in the range (1–3) $\times 10^{13}$ cm^{-3} (as determined in the titrations described later). The ≈100:1 ratio of HNO_3 to NO_3 ensured that there was minimal formation of FO via reaction 4,

$$F + NO_3 \rightarrow FO + NO_2 \quad (4)$$

NO_3 concentrations were determined by titration with NO:

$$NO_3 + NO \rightarrow 2NO_2 \quad (5)$$

with $k_5 = 2.6 \times 10^{-11}$ cm^3 s^{-1}.[18] For this purpose, measured flows of NO (2.0% in N_2) were added down the injector of the flow tube. The injector tip was placed 20 cm downstream of the F_2 discharge and 30 cm upstream of the detection region, allowing sufficient time for reaction 5 to go to completion. The O(^{3}P) resonance fluorescence (rf) signal resulting from NO_3 photolysis was monitored as a function of added NO; the [NO_3] was determined as the zero crossing of a plot of O(^{3}P) signal versus [NO].

In some experiments, absolute NO_3 quantum yields were determined using ozone photolysis to normalize for laser energy and rf detector sensitivity. For these experiments, the ozone was produced by flowing O_2 through an electrical discharge and was collected on a silica gel trap cooled to dry ice temperature. The ozone was added to the flow tube by diverting the main He flow through the silica gel trap. The O_3/He flow was passed through a 3-cm-long cell, and [O_3] was monitored by absorption at 253.7 nm using a filtered Hg pen ray lamp as the light source. Ozone concentrations in the flow tube were in the range (7–35) $\times 10^{14}$ molecules cm^{-3}.

Photolysis was accomplished using a dye laser (Spectra Physics) pumped by a pulsed excimer laser (Questek Model 2440). The excimer laser was triggered by a delay generator, usually at 11 Hz. The delay generator was also used to pretrigger the multichannel analyzer board, typically 5 ms before the laser pulse. The excimer laser energy was 90–120 mJ/pulse, as determined by an energy meter (Questek Model P9104). The excimer beam was used to pump one of three dyes: Rhodamine 6G (570–598 nm), Rhodamine 610 (589–619 nm), and Kiton Red (609–635 nm). The dye laser energy (as monitored by the energy meter) was between 0.1 and 2 mJ/pulse at the cell, depending on the dye and the wavelength. The unfocused laser beam, approximately 1 cm^2 in size, was directed into the photolysis cell at a 45° angle to the direction of gas flow.

Resonance lamps, directed at right angles to the photolysis laser, were used to excite fluorescence in the O(^{3}P) (near 130 nm)[19] or NO (in the γ bands near 226 nm)[12] photoproducts. For O(^{3}P) excitation, the lamp consisted of a microwave discharge in about 0.5 Torr of ultrahigh purity (UHP) helium, which typically contains ppm levels of O_2 impurity. For NO, about 2 Torr of air was discharged. The lamps were 12 cm long and 0.9 cm i.d. and were constructed of Pyrex. The interface between the lamps and the photolysis cell was a MgF_2 window. Gases were flowed into the front end of the lamp to avoid absorption of the resonance radiation by O(^{3}P) or NO produced in the lamp. Fluorescence signals were focused by a plano-convex lens (MgF_2 for O(^{3}P), quartz for NO) onto the entrance window of a photomultiplier tube (PMT): Hamamatsu R1459 for O(^{3}P) or Hamamatsu R374 for NO. The lens also acted as the interface between the PMT housing and the photolysis region. The PMTs were located at right angles to both the laser and the lamps, approximately 25 cm from the photolysis region. The region between the lens and the PMT was equipped with a series of baffles to limit scattered radiation. For O(^{3}P) detection, a CaF_2 window (cutoff near 125 nm) was placed in front of the PMT to eliminate potential interferences from Lyman-α radiation (122 nm), and the collection region was purged with a slow flow of UHP N_2 to limit absorption of the 130-nm radiation by O_2.[19] For NO, a band-pass filter (25-nm bandwidth centered at 215 nm) was employed to limit the wavelength region seen by the PMT.

The fluorescence signal was processed by an amplifier/discriminator (Pacific Instruments) and transferred to an IBM-PC equipped with an EG&G ACE multichannel scaler for collecting the time-resolved fluorescence signals. Typically, 100 laser shots were summed to obtain the O(^{3}P) signal from NO_3, while 500–2500 shots were summed for O_3. For NO detection,

10 000 laser shots were typically used. The detection limits for NO_3 photolysis experiments were $\approx 10^9$ atom cm^{-3} for $O(^3P)$ and $\approx 2 \times 10^{11}$ molecules cm^{-3} for NO.

Results and Discussion

The observed $O(^3P)$ rf signals were found to rise very rapidly following the laser pulse (<1 μs) and then to decay away on the time scale of a 1-2 ms. The time evolution of the observed rf signals was identical for photolysis of NO_3 and O_3 for a given pressure and flow rate and was probably dominated by diffusion and/or linear flow of the gases out of the detection region. Chemical loss of $O(^3P)$ due to reaction with NO_3 or with O_3 is expected to be slower, 10–50 ms, for typical conditions employed here.

Absolute $O(^3P)$ quantum yields from NO_3 photolysis (ϕ_1) were obtained using O_3 to normalize for laser power and rf detection sensitivity:

$$O_3 + h\nu \rightarrow O(^3P) + O_2(^3\Sigma_g^-) \qquad (6)$$

O_3 and then NO_3 were photolyzed separately in back-to-back experiments. For the O_3 photolyses, conditions in the flow tube were unchanged from the NO_3 experiment, except that the discharge was turned off. In this way, the HNO_3 concentration was approximately constant in both experiments and changes in rf lamp intensity due to HNO_3 absorption were minimized. Ozone itself may have absorbed the resonance lamp radiation to a small extent, since a 5–10% decrease in the background signal was observed on addition of O_3. This effect was corrected for by normalizing to the ratio of background signals (BG_{O_3}/BG_{NO_3}), as shown in the equation below. Blank runs conducted with and without F_2 flowing showed that there was no measurable absorption of the O atom resonance radiation at the levels of F_2 used. The signal (S) was obtained as the difference between the peak signal (immediately following the laser pulse) and the average background signal before the pulse. NO_3 quantum yields were then obtained as follows:

$$\phi_1 = \frac{S_{NO_3}}{S_{O_3}} \frac{\sigma_{O_3}}{\sigma_{NO_3}} \frac{[O_3]}{[NO_3]} \frac{BG_{O_3}}{BG_{NO_3}} \phi_6$$

O_3 absorption cross sections (σ_{O_3}) in the Chappuis bands were obtained from Anderson and Mauersberger[20] while the O_3 quantum yield (ϕ_6) was taken as unity at all wavelengths.[21] NO_3 absorption cross section (σ_{NO_3}) were taken from the recommendations of Wayne *et al.*[1] The NO_3 concentration was determined by titration with NO, while the O_3 concentration was determined by UV absorption at 253.7 nm as discussed earlier. The absolute NO_3 quantum yields obtained in this fashion were 1.06 ± 0.15 at 582 nm, 0.72 ± 0.12 at 590 nm, and 0.52 ± 0.07 at 603 nm (uncertainties are precision only). The largest experimental uncertainty lies in the variability of the $O(^3P)$ signals obtained in the O_3 photolyses. Back-to-back photolyses of O_3 yielded signals which varied by ±10%; this variability is most likely due to drift in the ozone concentration during the course of the photolysis and to noise in the $O(^3P)$ signals. Additional systematic uncertainties lie in the NO_3 absorption cross sections (±10%) and in the O_3 cross sections (±5%), leading to an overall uncertainty in the final quantum yields of about 25%.

A series of experiments were then conducted to deterine the relative $O(^3P)$ quantum yields as a function of wavelength. Typically, the rf signal (S) was summed over 100 laser shots at each wavelength and corrected for the background signal as discussed above. Relative $O(^3P)$ quantum yields (ϕ_{1,λ_i}) as a function of wavelength were then obtained as follows:

$$\frac{\phi_{1,\lambda_1}}{\phi_{1,\lambda_2}} = \frac{S_{\lambda_1}}{S_{\lambda_2}} \frac{I_{\lambda_2}}{I_{\lambda_1}} \frac{\sigma_{\lambda_2}}{\sigma_{\lambda_1}}$$

where the S_{λ_i} are the background-corrected rf signals at wavelength λ_i, the σ_{λ_i} are the absorption cross section at λ_i,[1] and the I_{λ_i} are the laser power at λ_i. Typically, 10–15 data points were collected over the course of about a half hour and were normalized in the manner described above. Multiple measurements were made at a particular wavelength throughout the course of a measurement set to check for possible changes in $[NO_3]$. In all cases, the multiple measurements agreed within experimental error (±5%), ensuring that no significant changes in $[NO_3]$ had occurred.

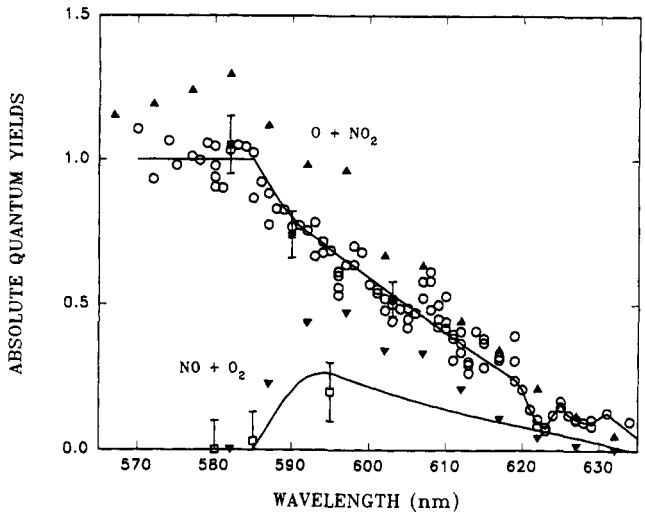

Figure 2. *Quantum yields for NO_3 photolysis:* (○) *relative $O(^3P)$ quantum* yields, this study; (■) absolute $O(^3P)$ quantum yields obtained relative to O_3 photolysis, this study; (□) absoltue NO quantum yields, this study; (—) recommended $O(^3P)$ (upper) and NO (lower) quantum yields, this work; (▲) $O(^3P)$ quantum yields of Magnotta and Johnston;[12] (▼) NO quantum yields of Magnotta and Johnston.[12]

Because of changes in the resonance lamp intensity, $O(^3P)$ rf signals recorded from day to day could not be directly compared. Instead, successive data sets were recorded over overlapping wavelength regions and normalized to each other in the region of overlap.

The data obtained in this fashion (eight separate data sets) were then normalized using the results of the O_3 experiments above. Because the uncertainty in the absolute data point at 582 nm is greater than the relative measurements (because of the weaker $O(^3P)$ rf signals obtained from O_3 photolysis) and because the absolute yield is not significantly different from unity, the relative $O(^3P)$ data set has been normalized by averaging all data points between 570 and 585 nm and taking this value to be unity. The full $O(^3P)$ data set is shown in Figure 2, the open circles representing the relative measurements and the solid squares representing the measurements made relative to ozone. The recommended $O(^3P)$ yields as a function of wavelength are shown as the solid line in Figure 2 and are listed in Table I.

The $O(^3P)$ quantum yield is found to be approximately unity between 570 and 585 nm, decreasing to nearly undetectable levels near 635 nm. The decrease in $O(^3P)$ yield with wavelength is essentially linear between 585 and 635 nm, except in the region of the strong 1–0 NO_3 absorption near 623 nm, where the quantum yield drops significantly below the expected value. It appears as though absorption in this strong 1–0 transition does not lead to $O(^3P)$ production but may lead predominantly to fluorescence. This is perhaps not surprising since absorption in this band is promoting NO_3 from $v = 0$ in the ground state specifically to $v = 1$ in the upper state, which lies some 850 cm^{-1} below the barrier to dissociation to NO_2 and $O(^3P)$, and so direct dissociation is unlikely.

The $O(^3P)$ quantum yield data set can be compared with the work of Magnotta and Johnston,[12] as shown in Figure 2. Using the currently recommended NO_3 absorption cross sections[1] and the cross section/quantum yield products reported by Magnotta

TABLE I: Recommended Quantum Yields for NO_3 Photodissociation at 298 K as a Function of Wavelength

λ	ϕ_1	ϕ_2	λ	ϕ_1	ϕ_2
586	0.958	0.042	613	0.350	0.121
587	0.916	0.084	614	0.332	0.115
588	0.874	0.126	615	0.314	0.109
589	0.832	0.168	616	0.296	0.103
590	0.801	0.199	617	0.278	0.098
591	0.770	0.230	618	0.261	0.092
592	0.750	0.250	619	0.243	0.086
593	0.729	0.259	620	0.209	0.081
594	0.709	0.265	621	0.141	0.076
595	0.690	0.265	622	0.095	0.070
596	0.670	0.255	623	0.076	0.065
597	0.650	0.245	624	0.122	0.060
598	0.631	0.236	625	0.159	0.054
599	0.611	0.226	626	0.122	0.049
600	0.592	0.217	627	0.106	0.043
601	0.573	0.209	628	0.096	0.038
602	0.554	0.200	629	0.095	0.032
603	0.534	0.192	630	0.112	0.026
604	0.516	0.184	631	0.130	0.019
605	0.497	0.176	632	0.108	0.013
606	0.478	0.169	633	0.087	0.005
607	0.459	0.161	634	0.066	0.000
608	0.441	0.154	635	0.045	0.000
609	0.422	0.147	636	0.020	0.000
610	0.404	0.141	637	0.010	0.000
611	0.386	0.134	638	0.000	0.000
612	0.368	0.128	639	0.000	0.000

and Johnston,[12] $O(^3P)$ quantum yields in excess of unity are obtained for $550 < \lambda < 590$ nm. In addition, the $[NO_3]$ in their experiments was inferred from measurements of $[NO_2]$ and $[N_2O_5]$ and from the equilibrium $N_2O_5 \rightleftharpoons NO_3 + NO_2$. However, the equilibrium constant employed by Magnotta and Johnston[12] is some 25% larger than the currently accepted value,[1,18] implying that $[NO_3]$ could have been 25% less than calculated and that the reported quantum yields may have been underestimated by some 25%. This would, of course, make the deviation from unity even larger. The most probable reason for the discrepancy is that the temperature in the photolysis region of the experiments of Magnotta and Johnston[12] was somewhat higher than the region in which $[NO_2]$ and $[N_2O_5]$ were determined. Hence, $[NO_3]$ may have been higher in the photolysis region than calculated, leading to a systematic overestimation of the measured ϕ. Clearly, from our measurements, the $O(^3P)$ quantum yield is not significantly different from unity between 570 and 585 nm.

Quantum yields for NO production from NO_3 photolysis were estimated at certain wavelengths. NO yields were calculated by measuring the rf signal of a known amount of NO which was added to the flow tube. This method of NO yield calculation should be regarded as semiquantitative in nature since the NO signal is calibrated with room temperature NO whereas the NO photoproduct may be produced in excited rovibrational levels and hence have different rf sensitivities. Also, the NO generated photolytically will have a different spatial distribution to the NO flow used for calibration.

NO was detected as a product of NO_3 photolysis at 590 nm, with an approximate quantum yield of 20%, while no NO signal was seen at 580 and 585 nm, implying a yield of less than 10%. While these yields are only semiquantitative in nature, they are consistent with the $O(^3P)$ yields discussed above ($\phi_1 \approx 1$ at 580 and 585 nm and $\phi_1 \approx 0.8$ at 590 nm). These NO yields are also in general agreement with the work of Magnotta and Johnston,[12] who obtained NO yields of 0 at 580 nm and 0.30 at 590 nm. While the NO yields reported by Magnotta and Johnston[12] may be overestimated for the same reasons as discussed above for ϕ_1, the accuracy of our NO yield data is insufficient to test this hypothesis. Our best estimates of ϕ_2 as a function of wavelength, as shown in Figure 2, were obtained using the ratio of $(\phi_2/\phi_1)_{MJ}$ measured by Magnotta and Johnston, normalizing their data

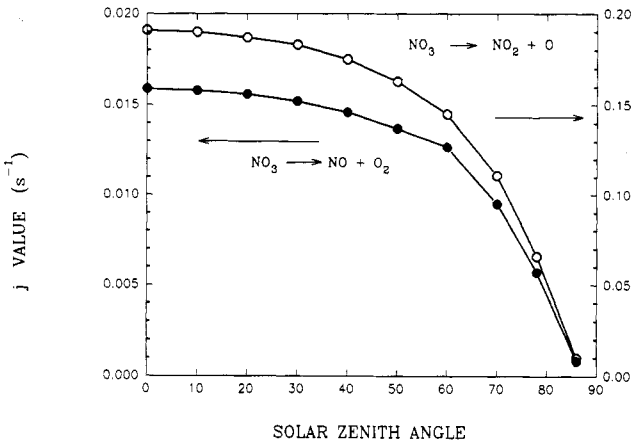

Figure 3. Photolysis rates (j_1 and j_2) for NO_3 as a function of solar zenith angle at sea level.

using the current ϕ_1 estimates at each wavelength: $\phi_2 \approx (\phi_2/\phi_1)_{MJ}(\phi_1)_{NCAR}$.

The ϕ_1 measured here and the ϕ_2 obtained as outlined above (both summarized in Table I) can be employed to calculate the atmospheric photolysis rate for reactions 1 and 2. These quantum yield data were coupled with the 298 K cross section data of Wayne *et al.*[1] and the solar flux data of Demerjian *et al.*[22] (best estimate albedo) to estimate the j_1 and j_2 values for NO_3 at 298 K at various solar zenith angles (Figure 3). The j_1 and j_2 values for overhead sun ($j_1 = 0.19\ s^{-1}$, $j_2 = 0.016\ s^{-1}$) are in general agreement with the estimates of Madronich[23] ($j_1 = 0.17\ s^{-1}$, $j_2 = 0.021\ s^{-1}$), who adjusted the Magnotta and Johnston data set such that the total quantum yield did not exceed unity. They also agree well with the original photolysis rate calculations of Magnotta and Johnston[12] ($j_1 = 0.18 \pm 0.06\ s^{-1}$; $j_2 = 0.022 \pm 0.007\ s^{-1}$). It should be noted that these j_2 values are based on the normalization procedure discussed above; more quantitative determinations of the NO quantum yields as a function of wavelength are desirable.

The wavelength dependence of the $O(^3P)$ quantum yield data can be used to infer the $\Delta H_{f,298}$ of NO_3, if it is assumed that the barrier for dissociation of NO_3 to NO_2 and $O(^3P)$ is located between 580 and 585 nm and that dissociation at longer wavelengths occurs with the aid of internal energy in the NO_3. While a quantitative determination of $\Delta H_{f,298}$ for NO_3 cannot be made from an analysis of our room temperature quantum yield data because of the contribution of internal energy to the dissociation, a dissociation threshold of 580–585 nm implies a $\Delta H_{f,298}$ for NO_3 of 18 ± 1 kcal/mol.

Early determinations of $\Delta H_{f,298}$ for NO_3,[2,24,25] based on the temperature dependence of the equilibrium constant for the $NO_2 + NO_3 \rightleftharpoons N_2O_5$ system and a $\Delta H_{f,298}$ of 2.7 kcal/mol for N_2O_5,[26,27] yielded values near 17.5 kcal/mol. However, McDaniel *et al.*,[28] based on their measurement of the ΔH_{vap} of N_2O_5 and ΔH_{soln} for $N_2O_5(s)$ in water, determined ΔH_f for N_2O_5 to be 1.2 kcal/mol. This redetermination led them to conclude that the enthalpy of formation for NO_3 was lower than previously believed, 15.4 ± 0.8 kcal/mol. This value, which was adapted by Wayne *et al.*[1] in their recent review, corresponds to a wavelength threshold for $O(^3P)$ production near 548 nm, in disagreement with the threshold observed in our work and in that of Magnotta and Johnston.[12] More convincingly, photodissociation studies of NO_3 in a molecular beam apparatus have recently been conducted by Davis *et al.*[29] In these experiments, the NO_3 is rotationally cold and the dissociation threshold can be much more accurately determined than in our experiments. Davis *et al.* report a $\Delta H_{f,298}$ of 17.6 kcal/mol for NO_3, a value consistent with our data. Also, Weaver *et al.*[30] obtained a value of 17.9 kcal/mol for the $\Delta H_{f,298}$ of NO_3 from a study of the photoelectron spectroscopy of NO_3^-. We recommend the use of a value of 17.7 kcal/mol for the $\Delta H_{f,298}$

of NO_3, an average of the two direct measurements.[29,30] The results of these absolute determinations give a $\Delta H_{f,298}$ for N_2O_5 of close to 2.7 kcal/mol, agreeing favorably with that of Ray and Ogg[26] rather than the lower value (1.2 kcal/mol) of McDaniel *et al.*[28] Since the heat of vaporization of N_2O_5 determined by McDaniel *et al.* agrees well with previous determinations,[31] the discrepancy apparently lies in the N_2O_5 heat of solution measurement of McDaniel *et al.*

Conclusions

In this paper, we have reported quantitative $O(^3P)$ quantum yields from NO_3 photolysis between 570 and 635 nm. The $O(^3P)$ yield was found to be unity from 570 to 585 nm, clarifying the results of previous work which indicated a quantum yield of greater than one. The $O(^3P)$ yield was found to decrease beyond 585 nm to a value of less than 0.1 at 635 nm. Anomalously low $O(^3P)$ yields were found in the region of the strong absorption band near 623 nm, where fluorescence likely dominates. Qualitative NO quantum yields have also been obtained, with ϕ_{NO} of less than 10% at 580 nm and about 20 ± 10% at 590 nm being obtained. The quantum yield data were used to obtain atmospheric dissociation rates for NO_3: $j_1 = 0.19\ s^{-1}$ and $j_2 = 0.016\ s^{-1}$ for overhead sun and clear sky conditions at sea level. The wavelength dependence of the $O(^3P)$ quantum yields imply a $\Delta H_{f,298}$ of 18 ± 1 kcal/mol for NO_3, in agreement with recent direct determinations.[29,30]

Acknowledgment. This work was carried out with the partial support of the NASA Upper Atmosphere Research Program, Contract W-16042. The authors thank H. Floyd Davis for communicating results prior to publication and Thomas Staffelbach and Frank Flocke for helpful comments regarding the manuscript. The National Center for Atmospheric Research is supported by the National Science Foundation.

References and Notes

(1) Wayne, R. P.; Barnes, I.; Biggs, P.; Burrows, J. P.; Canosa-Mas, C. E.; Hjorth, J.; LeBras, G.; Moortgat, G. K.; Perner, D.; Poulet, G.; Restelli, G.; Sidebottom, H. *Atmos. Environ.* **1991**, *25A*, 1–203.

(2) Graham, R. A.; Johnston, H. S. *J. Phys. Chem.* **1978**, *82*, 254–268.

(3) Mitchell, D. N.; Wayne, R. P.; Allen, P. J.; Harrison, R. P.; Twin, R. J. *J. Chem. Soc., Faraday Trans. 2* **1980**, *76*, 785–793.

(4) Marinelli, W. J.; Swanson, D. M.; Johnston, H. S. *J. Chem. Phys.* **1982**, *76*, 2864–2870.

(5) Ravishankara, A. R.; Wine, P. H. *Chem. Phys. Lett.* **1983**, *101*, 73–78.

(6) Cox, R. A.; Barton, R. A.; Ljungström, E.; Stocker, D. W. In *Physicochemical behaviour of atmospheric pollutants, Air pollution report no. 3*; Versino, B., Angeletti, G., Eds.; D. Reidel Publishing: Dordrecht, 1984; pp 205–215.

(7) Burrows, J. P.; Tyndall, G. S.; Moortgat, G. K. *J. Phys. Chem.* **1985**, *89*, 4848–4856.

(8) Sander, S. P. *J. Phys. Chem.* **1986**, *90*, 4135–4142.

(9) Ravishankara, A. R.; Mauldin, R. L. III. *J. Geophys. Res.* **1986**, *91*, 8709–8712.

(10) Canosa-Mas, C. E.; Fowles, M.; Houghton, P. J.; Wayne, R. P. *J. Chem. Soc., Faraday Trans. 2*, **1987**, *83*, 1465–1474.

(11) Cantrell, C. A.; Davidson, J. A.; Shetter, R. E.; Anderson, B. A.; Calvert, J. G. *J. Phys. Chem.* **1987**, *91*, 5858–5863.

(12) Magnotta, F.; Johnston, H. S. *Geophys. Res. Lett.* **1980**, *7*, 769–772.

(13) Nelson, H. H.; Pasternack, L.; McDonald, J. R. *J. Phys. Chem.* **1983**, *87*, 1286–1288.

(14) Nelson, H. H.; Pasternack, L.; McDonald, J. R. *J. Chem. Phys.* **1983**, *79*, 4279–4284.

(15) Ishiwata, T.; Fujiwara, I.; Naruge, Y.; Obi, K.; Tanaka, I. *J. Phys. Chem.* **1983**, *87*, 1349–1352.

(16) Tyndall, G. S.; Orlando, J. J.; Cantrell, C. A.; Shetter, R. E.; Calvert, J. G. *J. Phys. Chem.* **1991**, *95*, 4381–4386.

(17) Orlando, J. J.; Tyndall, G. S.; Cantrell, C. A.; Calvert, J. G. *J. Chem. Soc., Faraday Trans.* **1991**, *87*, 2345–2349.

(18) DeMore, W. B.; Sander, S. P.; Golden, D. M.; Hampson, R. F.; Kurylo, M. J.; Howard, C. J.; Ravishankara, A. R.; Kolb, C. E.; Molina, M. J. *Chemical Kinetics and Photochemical Data for Use in Stratospheric Modeling, Evaluation No. 10*; JPL Publication 92–20, California Institute of Technology, Pasadena, CA.

(19) Wine, P. H.; Ravishankara, A. R. *Chem. Phys. Lett.* **1981**, *77*, 103–109.

(20) Anderson, S. M.; Mauersberger, K. *Geophys. Res. Lett.* **1992**, *19*, 933–936.

(21) Calvert, J. G.; Pitts, J. N., Jr. *Photochemistry*; John Wiley and Sons: New York, 1966.

(22) Demerjian, K. L.; Schere, K. L.; Peterson, J. T. in *Advances in Environmental Science and Technology*; Pitts, J. N.; Metcalf, R., Eds.; John Wiley and Sons: New York, 1980.

(23) Madronich, S. Unpublished results quoted in ref 1.

(24) Kircher, C. C.; Margitan, J. J.; Sander, S. P. *J. Phys. Chem.* **1984**, *88*, 4370–4375.

(25) Burrows, J. P.; Tyndall, G. S.; Moortgat, G. K. *Chem. Phys. Lett.* **1985**, *119*, 193–198.

(26) Ray, J. D.; Ogg, R. A., Jr. *J. Phys. Chem.* **1957**, *61*, 1087–1088.

(27) Stull, D. R.; Prophet, H. *JANAF Thermochemical Tables*, 2nd ed.; **1971**, *NSRDS-NB37*.

(28) McDaniel, A. H.; Davidson, J. A.; Cantrell, C. A.; Shetter, R. E.; Calvert, J. G. *J. Phys. Chem.* **1988**, *92*, 4172–4175.

(29) Davis, H. F.; Kim, B.; Johnston, H. S.; Lee, Y. T. *J. Phys. Chem.* **1993**, *97*, 2172–2180.

(30) Weaver, A.; Arnold, D. W.; Bradforth, S. E.; Neumark, D. M. *J. Chem. Phys.* **1991**, *94*, 1740–1751.

(31) Daniels, F.; Bright, A. C. *J. Am. Chem. Soc.* **1920**, *42*, 1131.